

Published in final edited form as:

Anal Biochem. 2012 February 15; 421(2): 489–498. doi:10.1016/j.ab.2011.11.021.

Fluorescent reporters of thrombin, heparin cofactor II, and heparin binding in a ternary complex

Ingrid M. Verhamme*

Department of Pathology, Microbiology, and Immunology, Vanderbilt University School of Medicine, Nashville, TN 37232, USA

Abstract

Thrombin inactivation by heparin cofactor II (HCII) is accelerated by ternary complex formation with heparin. The novel active-site-labeled thrombins, [4'F]FPR-T and [6F]FFR-T, and the exosite I probe, Hir-(54–65)(SO₃⁻), characterized thrombin exosite I and II interactions with HCII and heparin in the complex. HCII binding to exosite I of heparin-bound [4'F]FPR-T caused a saturable fluorescence increase, absent with antithrombin. Heparin binding to exosite II and a second weaker site caused fluorescence quenching of [6F]-FFR-T, attenuated by simultaneous Hir-(54–65)(SO₃⁻) binding. Stopped-flow analysis demonstrated ordered assembly of HCII and the [6F]FFR-T-heparin complex, in agreement with tighter heparin binding to thrombin than to HCII. Saturating HCII dependences and bell-shaped heparin dependences of the fluorescence change reported ternary complex formation, consistent with a template mechanism in which the thrombin-heparin complex binds HCII and allowing for interaction of thrombin·(heparin)₂ complexes with HCII. Hir-(54–65)(SO₃⁻) displacement in reactions with FPR-blocked and active thrombin indicated a concerted action of the active site and exosite I during ternary complex formation. These studies demonstrate that binding of HCII to the thrombin-heparin complex is dramatically enhanced compared with heparin binding alone and that exosite I is still available for ligand or HCII binding when both heparin binding sites on thrombin are saturated.

Keywords

Serpins; Heparin cofactor II; Thrombin inactivation; Heparin; Fluorescence equilibrium binding; Stopped-flow fluorescence

The circulatory serpins (serine proteinase inhibitors),¹ heparin cofactor II (HCII) and antithrombin (AT), inactivate the central coagulation proteinase, α-thrombin (T), in reactions accelerated by high-molecular-weight (*M_p*) heparin (Hep), a sulfated glycosaminoglycan (GAG) on the surface of vascular endothelial cells [1–4]. Thrombin inactivation by AT is critical in venous thrombosis and disseminated intravascular coagulation (DIC) [5], whereas HCII inhibits arterial thrombosis [6] and may protect against

© 2011 Elsevier Inc. All rights reserved.

*Fax: +1 615 343 7023. ingrid.verhamme@vanderbilt.edu.

¹*Abbreviations used:* serpin, serine proteinase inhibitor; HCII, heparin cofactor II; AT, antithrombin; T, α-Thrombin; *M_p*, molecular weight; Hep, heparin; GAG, glycosaminoglycan; DIC, disseminated intravascular coagulation; Hir, hirudin peptide; Hir-(54–65)(SO₃⁻), Gly-Asp-Phe-Glu-Glu-Ile-Pro-Glu-Glu-Tyr(SO₃⁻)-Leu-Gln; [4'F]FPR-T, [4'-[(acetyl)amino]methyl]fluorescein]-D-Phe-Pro-Arg-thrombin; [6F]FFR-T, [6-(acetamido)fluorescein]-D-Phe-Phe-Arg-thrombin; F2, fragment 2; S2238, H-D-Ile-Pro-Arg-p-nitroanilide; Chromozym TH, Tos-Gly-Pro-Arg-P-nitroanilide; 6-IAF, 6-(iodoacetamido)fluorescein; 4'-IAF, 4'-[(iodoacetyl)amino]methyl]fluorescein; ATA-FPR-CH₂Cl, N^α-[(acetylthio)acetyl]-D-Phe-Pro-Arg-CH₂Cl; ATA-FFR-CH₂Cl, N^α-[(acetylthio)acetyl]-D-Phe-Phe-Arg-CH₂Cl; SDS, sodium dodecyl sulfate; FPR-CH₂Cl, D-Phe-Pro-Arg-CH₂Cl; PEG, polyethylene glycol; pNA p-nitroaniline; DS, dermatan sulfate.

atherosclerosis [7,8] and DIC associated with inflammatory diseases [9] and certain cancers [10]. Heparin forms a reversible ternary complex intermediate with thrombin and the serpins, followed by serpin cleavage and extensive conformational rearrangement of the covalent thrombin-serpin complex [1,11]. The order of assembly of ternary complexes of thrombin, heparin, and the serpins depends on the type of heparin and on the differences in dissociation constants of the binary heparin complexes with thrombin and with the serpins. Heparin with high affinity for AT contains a specific sulfated pentasaccharide sequence [12,13] and binds AT with $K_{AT,Hep} \sim 0.02 \mu\text{M}$ [14], whereas low-affinity heparin, lacking such a sequence, binds AT 1000-fold weaker, with $K_{AT,Hep} \sim 20 \mu\text{M}$ [15]. Both types of heparin bind HCII with similar affinity, with $K_{HCII,Hep} = 15$ to $40 \mu\text{M}$ [16,17]. Thrombin binding by these heparins was reported to be indistinguishable, with $K_{T,Hep} = 0.7$ to $0.9 \mu\text{M}$ [1,15], although binding constants for high-affinity heparin ranging from 0.02 to $0.07 \mu\text{M}$ have been observed [16,18].

Thrombin possesses two lysine- and arginine-rich sites, exosites I and II [19,20], with different specificities of ligand binding. Exosite I binds the natural thrombin substrate, fibrinogen; the acidic C-terminal region of the thrombin inhibitor, hirudin [21]; and the hirudin-like Glu53-Asp75 acidic region in the N terminus of HCII, absent in AT [3,4,22-26]. This acidic region in HCII is presumed to be cryptic in the absence of heparin and hypothesized to become available for interaction with exosite I by a conformational change triggered by binding of heparin to HCII helix D [3,26]. Thrombin exosite II binds high- and low- M_r heparins [20,27,28]. High- M_r heparin forms a bridge between thrombin and the heparin binding sites on HCII [29] and AT [30,31]. The T-Hep-HCII complex, stabilized both by the exosite I-HCII contact and by heparin bridging, has a tighter affinity than the T-Hep-AT ternary complex intermediate, as determined indirectly by kinetic analysis [15,16]. Heparin binding to the serpins and thrombin is assumed to obey rapid equilibrium kinetics [1,32]. Due to the large difference in affinity of AT and HCII for high-affinity heparin, the binary AT-Hep intermediate is saturated at heparin concentrations of approximately $0.2 \mu\text{M}$, whereas population of the HCII-Hep intermediate becomes significant only at much higher heparin concentrations, in the range of $K_{HCII,Hep}$, resulting in different preferred pathways of assembly of the ternary complex with thrombin [1,15,16]. Semi-logarithmic, bell-shaped heparin dependences of the inactivation rate constants for the thrombin-HCII reaction are very similar to those for the thrombin-AT reaction catalyzed by low-affinity heparin [15-17], with the ascending limb representing saturation of the binary T-Hep complex, which recruits free serpin, and the descending limb consistent with heparin saturation of the serpin. The currently accepted mechanism of heparin enhancement of HCII inhibitory activity proposes that the allosteric, heparin-induced release of the HCII N-terminal tail results in exosite I binding and formation of the ternary complex by binding of the HCII-Hep binary complex to thrombin. However, the heparin concentration range at which maximal thrombin inactivation is observed, 1 to $5 \mu\text{M}$, is sufficiently high to saturate binding to thrombin but not to HCII, which argues against a mechanism using the pathway of the HCII-Hep binary complex recruiting free thrombin to form the ternary complex. The mechanism is further compounded by the fact that thrombin is capable of binding multiple heparin molecules, and at least one additional GAG binding site, distinct from exosite II, was demonstrated by us and by others [16,33-38]. Saturation of an additional heparin binding site in or near exosite I was suggested to attenuate the rate of thrombin inactivation by HCII [39]; however, our published data indicate that exosite I of heparin-saturated thrombin ($\sim 200 \mu\text{M}$ heparin) is still capable of ligand binding [16].

The current study attempts to clarify these controversial issues of the HCII mechanism. The fluorescent thrombins [4'F]FPR-T and [6F]FFR-T, labeled with fluorescein at the active site, respectively allow selective characterization of exosite I and II contributions to ternary T-Hep-HCII complex formation, uncoupled from the inactivation chemistry, and report

quantitatively exosite binding as a result of thermodynamic exosite-active site linkage [40–42]. Heparin titrations of [6F] FFR-T also measure the affinity of a second heparin binding site on thrombin. Fluorescence equilibrium binding and stopped-flow experiments with these thrombins were combined with displacement of the exosite I binding peptide, Hir-(54–65)(SO₃⁻), during heparin-accelerated thrombin inactivation by HCII, and displacement of the fluorescently labeled peptide, [5F]Hir-(54–65)(SO₃⁻), from active-site-blocked FPR-thrombin, to compare exosite I involvement in ternary complex formation and during thrombin inactivation. These approaches are well-suited for studying the equilibrium binding steps of reversible ternary T-Hep-HCII complex assembly and quantitative characterization of the exosite I-HCII interaction. The results suggest that in an ordered pathway of ternary complex formation from T-Hep and HCII, the affinity of the T-Hep complex for HCII is dramatically increased compared with that of heparin alone, and allosteric triggering of HCII binding to exosite I may be facilitated by interaction of thrombin-bound, high-*M_r* heparin with the HCII GAG binding site. The affinity of the HCII N-terminal acidic domain for exosite I is higher in ternary complexes with active thrombin compared to active-site-blocked thrombin, consistent with participation of HCII binding to the active site, linked with exosite I binding. Our data also suggest that saturation of the T-(Hep)₂ complex does not exclude HCII binding to exosite I, and higher order intermediate complexes may play a role in heparin-accelerated thrombin inactivation by HCII.

Materials and methods

Proteins and materials

HCII, AT, and prothrombin were purified from human plasma [16,42,43]. α -Thrombin, prepared as described previously [42], was at least 90% active, determined by active site titration [44]. Prothrombin fragment 2 (F2) was prepared as described previously [41]. Protein concentrations were determined by absorbance at 280 nm with the respective absorption coefficients and molecular weights of 1.83 (mg/ml)⁻¹ cm⁻¹ and 36,700 for thrombin [45], 1.25 (mg/ml)⁻¹ cm⁻¹ and 12,900 for F2 [46], 0.59 (mg/ml)⁻¹ cm⁻¹ and 65,600 for HCII [47], and 0.65 (mg/ml)⁻¹ cm⁻¹ and 58,000 for AT [43]. Active HCII and AT concentrations were determined by stoichiometric titration with active-site-titrated thrombin. Heparin with *M_r* = 12,000 from porcine skin and Hir-(54–65)(SO₃⁻) were from Sigma. Low-*M_r* heparin (5000) from porcine intestinal mucosa was from Calbiochem. The monoclonal antibody against human thrombin exosite II was a gift from Douglas Tollefsen (Washington University) [48]. The chromogenic substrates S2238 and Chromo-zym TH were from Chromogenix and Roche, respectively. The fluorescence probes 5-carboxyfluorescein, 6-(iodoacetamido)fluorescein (6-IAF), and 4'-((iodoacetyl)amino)methyl)fluorescein (4'-IAF) were from Invitrogen. Active site labeling of thrombin and purification of the labeled species were performed as described previously [41,42]. Thrombin was inactivated with ATA-FPR-CH₂Cl or ATA-FFR-CH₂Cl by alkylation of the active site histidine, and the NH₂OH-generated thiol was labeled with 6-IAF or 4'-IAF to form [6F]FFR-T and [4'F]FPR-T, respectively. The purified labeled thrombins had a probe/thrombin active sites molar ratio of approximately 1 and migrated as single labeled bands on sodium dodecyl sulfate (SDS) polyacrylamide gels. FPR-thrombin was prepared by inactivation with FPR-CH₂Cl and was inactive in chromogenic substrate assays. [5F]Hir-(54–65)(SO₃⁻) was prepared by N-terminal labeling of Hir-(54–65)(SO₃⁻) with 5-carboxyfluorescein as described previously [11]. Equilibrium binding and kinetic studies were performed at 25 °C in 50 mM Hepes, 0.11 M NaCl, 5 mM CaCl₂, 1 mg/ml PEG (polyethylene glycol) 8000 (pH 7.4) buffer. Titrations of active-site-blocked thrombins contained 0.1 μ M FPR-CH₂Cl.

Fluorescence equilibrium binding of heparin, HCII, and Hir-(54–65)(SO₃⁻) to active-site-labeled thrombins

Heparin binding to [4′F]FPR-T and [6F]FFR-T, HCII binding to the labeled T·Hep complexes, and Hir-(54–65)(SO₃⁻) binding to the [6F]FFR-T·Hep complex were quantitated by measuring the change in probe fluorescence with an SLM 8100 or PTI spectrofluorometer, using acrylic cuvettes coated with PEG 20,000 to minimize protein adsorption. Titrations were performed as described previously [40], at the respective excitation and emission wavelengths 500 and 521 nm ([4′F]FPR-T) and 498 and 516 nm ([6F]FFR-T), with 8-nm bandpasses. Results were expressed as the fractional change in the initial fluorescence $[(F_{\text{obs}} - F_0)/F_0 = \Delta F/F_0]$, or the absolute change of $\Delta F/F_0$ ($\Delta\Delta F/F_0$), as a function of total titrant concentration and were fit by the appropriate binding equation for each experiment.

[4′F]FPR-T and [6F]FFR-T (10 and 20 nM final concentrations, respectively) were titrated with $M_r = 12,000$ heparin in pH 7.4 buffer. [4′F]FPR-T (10 nM) was also titrated with F2. Heparin dependences up to 1 to 2 μM and the F2 dependence were fit by the quadratic binding equation for binding of a single ligand [41]. Data sets that included higher heparin concentrations were fit by Eq. (1) for binding of two ligands, with the concentrations of the T·Hep and T·(Hep)₂ complexes calculated by simultaneous solution of the expressions for the equilibrium constants $K_{\text{T(Hep)}}$ and $K_{\text{T(Hep)2}}$ defined by the two-site model and the mass conservation equations. The fitted parameters were $K_{\text{T(Hep)}}$ for heparin binding to thrombin exosite II, $K_{\text{T(Hep)2}}$ for binding of a second heparin molecule, and the maximum fluorescence intensity changes $\Delta F_{\text{max,T(Hep)2}}/F_0$ and $\Delta F_{\text{max,T(Hep)2}}/F_0$:

$$\frac{\Delta F}{F_0} = \left(\frac{[\text{T} \bullet \text{Hep}]}{[\text{T}]_0} \right) \frac{\Delta F_{\text{max,T(Hep)2}}}{F_0} + \left(\frac{[\text{T} \bullet (\text{Hep})_2]}{[\text{T}]_0} \right) \frac{\Delta F_{\text{max,T(Hep)2}}}{F_0} \quad (1)$$

[6F]FFR-T (35 nM) was titrated with heparin in the absence and presence of fixed concentrations (5, 25, and 250 nM) of Hir-(54–65)(SO₃⁻) and with Hir-(54–65)(SO₃⁻) in the presence of 1.56 μM heparin. The data were analyzed simultaneously by models for two heparin binding sites on thrombin, in which binding of Hir-(54–65)(SO₃⁻) to thrombin exosite I is either competitive (Eq. (2)) or nonoverlapping with the second heparin binding site. Hir-(54–65)(SO₃⁻) binding in the absence of heparin was fluorescently silent. The fitted parameters for heparin binding to thrombin were as described above, and parameters for heparin binding to the T·Hir complex were $K_{\text{T(Hir)(Hep)}}$ and $\Delta F_{\text{max,T(Hir)(Hep)}}$:

$$\frac{\Delta F}{F_0} = \left(\frac{[\text{T} \bullet \text{Hep}]}{[\text{T}]_0} \right) \frac{\Delta F_{\text{max,T(Hep)2}}}{F_0} + \left(\frac{[\text{T} \bullet (\text{Hep})_2]}{[\text{T}]_0} \right) \frac{\Delta F_{\text{max,T(Hep)2}}}{F_0} + \left(\frac{[\text{T} \bullet \text{Hir} \bullet \text{Hep}]}{[\text{T}]_0} \right) \frac{\Delta F_{\text{max,T(Hir)(Hep)2}}}{F_0} \quad (2)$$

In the non-overlapping binding model, the fluorescence contribution of the T·(Hep)₂Hir complex formed by Hir binding to the T·(Hep)₂ complex is given by the term $([\text{T} \bullet (\text{Hep})_2 \bullet \text{Hir}]/[\text{T}]_0) \Delta F_{\text{max,T(Hep)2(Hir)2}}/F_0$ added to Eq. (2), with fitted parameters $K_{\text{T(Hep)2(Hir)2}}$ and $\Delta F_{\text{max,T(Hep)2(Hir)2}}/F_0$. Concentrations of the T·Hir·Hep and T·(Hep)₂·Hir complexes were again calculated from the expressions for the equilibrium constants $K_{\text{T(Hir)(Hep)}}$ and $K_{\text{T(Hep)2(Hir)2}}$ defined by the respective competitive and nonoverlapping models and the mass conservation equations. The Hir-(54–65)(SO₃⁻) titration of [6F]FFR-T at 1.56 μM heparin was also analyzed separately by the quadratic binding equation for binding of a single ligand, with fitted parameters $K_{\text{T(Hep)(Hir)}}$ for Hir-(54–65)(SO₃⁻) binding to the T·Hep complex, and $\Delta F_{\text{max,T(Hep)(Hir)2}}/F_0$.

Titration of HCII binding to [4'F]FPR-T (10 nM) and [6F]FFR-T (35 nM) were performed at fixed heparin concentrations (0.5, 5, 50, 100, and 200 μM heparin for HCII titrations of [4'F]FPR-T and 1.6, 5.2, 13.5, and 47 μM heparin for HCII titrations of [6F]FFR-T). [4'F]FPR-T was also titrated with HCII at 5 μM heparin in the presence of saturating anti-exosite II monoclonal antibody (2.5 μM antibody sites) and at 77 μM low- M_r (5000) heparin. Titrations of AT binding to both labeled thrombins in the presence of heparin were included for comparison. Heparin dependences of [4'F]FPR-T, HCII, and heparin binding in a ternary complex were constructed by titration of [4'F]FPR-T with heparin at fixed concentrations of 0.36 and 2.6 μM HCII. A heparin dependence of $\Delta\Delta F/F_0$ of ternary complex formation with [6F]FFR-T and HCII was constructed by single cuvette measurements of sequential fluorescence changes caused by reacting [6F]FFR-T (72 nM) with varying heparin concentrations and a fixed concentration of HCII (0.38 μM). The effect of Hir-(54–65)(SO_3^-) on ternary complex formation of [6F]FFR-T with heparin and HCII was measured by HCII titrations of [6F]FFR-T (35 nM) in the presence of 1.6 μM heparin and 25 and 250 nM Hir-(54–65)(SO_3^-). All fluorescence measurements were corrected for dilution and background scattering (<10%). Heparin and HCII dependences of the fluorescence changes were analyzed by models of ternary T·Hep·HCII complex formation that respectively included and excluded participation of the quaternary T·(Hep)₂HCII complex. Hir-(54–65)(SO_3^-) binding to exosite I in the reactions of [6F]FFR-T with HCII and 1.6 μM heparin was analyzed by the same models, with appropriate fixing of the binding constants for the quaternary interactions determined by the heparin and HCII dependences.

[5F]Hir-(54–65)(SO_3^-) release from FPR-thrombin in presence of heparin and HCII

In separate experiments, [5F]Hir-(54–65)(SO_3^-) (52 nM) was incubated with 200 nM FPR-thrombin and 0.9 or 1.5 μM HCII and was titrated with heparin. In a comparison experiment, 0.5 μM AT was used instead of HCII. The excitation and emission wavelengths were 491 and 520 nm [49], respectively, with 4-nm band-passes. Measurements were corrected for dilution and background scattering (<10%). The heparin dependences were analyzed both by the cubic equation (adapted from Ref. [11]) for competitive binding of HCII and the peptide to the T·Hep complex, with the concentration of the latter calculated from the equilibrium and mass balance expressions, and by a hyperbolic dependence of fluorescence change (Eq. (3)):

$$F_{\text{obs}} = \frac{F_{\text{lim}}[\text{HCII}]_{\text{free}}}{K_{\text{app,T(H)(HCII)}} \left(1 + K_{\text{T(Hep)}} / [\text{Hep}]_{\text{free}} \right) + [\text{HCII}]_{\text{free}}}, \quad (3)$$

with $[\text{HCII}]_{\text{free}}$ and $[\text{Hep}]_{\text{free}}$ calculated from the mass balances and the fitted dissociation constants $K_{\text{T(Hep)}}$ for the T·Hep complex and an apparent dissociation constant $K_{\text{app,T(H)(HCII)}}$ for the ternary complex including the effect of competitive [5F]Hir-(54–65)(SO_3^-) binding. The fixed parameters F_{lim} and the K_D for peptide binding to T·Hep were determined independently as published previously [16,49].

Effect of Hir-(54–65)(SO_3^-) on heparin-accelerated thrombin inactivation by HCII

Heparin-accelerated thrombin inactivation (1 and 50 μM heparin, 1–10 nM thrombin) by HCII (0.36 μM) in the absence and presence of increasing concentrations of Hir-(54–65)(SO_3^-) was monitored by continuous competitive chromogenic substrate hydrolysis under first-order conditions of chromogenic substrate, S2238 or ChromozymTH (100 μM) and HCII. [16,50,51]. Respective K_m and k_{cat} values for S2238 hydrolysis were 1.5 μM and 90 s^{-1} [52], and those for Chromozym TH hydrolysis were 11 μM and 176 s^{-1} [34]. Under our

experimental conditions, heparin had no significant effect on chromogenic substrate hydrolysis. Inactivation reactions were performed in pH 7.4 reaction buffer as described previously [34], and *p*-nitroaniline (*p*NA) formation was monitored continuously at 405 nm with a Shimadzu 2401 spectrophotometer. Time courses were fit by a two-exponential equation [16,34], with a fast first-order rate constant k_{obs} describing α -thrombin inactivation and a very slow rate constant for trace γ -thrombin inactivation [4]. The rate constants, corrected for chromogenic substrate competition, were calculated as $k = k_{obs}(1 + [S]_0/K_m)$, with $[S]_0$ and K_m the concentration and Michaelis constant for the chromogenic substrate. The Hir-(54–65)(SO₃⁻) concentration dependence of k was analyzed by a model that excludes simultaneous occupation of exosite I by the peptide and the HCII N-terminal acidic sequence (Scheme 1).

At 1 and 50 μ M heparin, thrombin was respectively present predominantly as T·Hep and T·(Hep)₂ complex. In Scheme 1, only the T·Hep_x-HCII complex contributes to the inactivation reaction. $K_{T(Hep)_x(Hir)}$ is the dissociation constant for Hir-(54–65)(SO₃⁻) binding to T·Hep_x, and $K_{T(Hep)_x(HCII)}$ is the dissociation constant for binding of T·Hep_x to HCII. The fractions of sites on T·Hep_x occupied by either HCII or Hir-(54–65)(SO₃⁻), were expressed in terms of the free ligand concentrations by simultaneous solution of two cubic equations [53], and the observed inactivation rate constant was a function of the T·Hep_x-HCII concentration. Least squares fitting of binding and kinetic data was performed with Scientist software (MicroMath). All reported estimates of error represent ± 2 standard deviations.

Stopped-flow kinetics of ternary complex formation between [6F]FFR-T, heparin, and HCII

Time traces (1000 data points, 3–5 s) of heparin binding to [6F]FFR-T, and of ternary complex formation with HCII, were acquired with an Applied Photophysics SX-18MV stopped-flow spec-trofluorometer in single mixing mode. Fluorescence changes were measured with excitation at 485 nm and a 495-nm emission cut-on filter (Melles-Griot). The reaction volume was 200 μ l, the path length was 2 mm, and experiments were performed at 25 °C in reaction buffer. In separate experiments, [6F]FFR-T (87 nM final) was reacted with buffer, heparin (0.32 μ M), or a mixture of heparin (0.32 μ M) and HCII (0.54 μ M). The order of addition was reversed by reacting a mixture of [6F]FFR-T and heparin with HCII at identical final reactant concentrations. Six time traces were averaged for each experiment. Control reactions containing buffer, heparin, and HCII and buffer and [6F]FFR-T were used to quantitate background and initial probe fluorescence, respectively, and to permit transformation of raw data into $\Delta F/F_0$. Time traces were analyzed by the appropriate single- or two-exponential equations [54].

Results

Fluorescence equilibrium binding of heparin and Hir-(54–65)(SO₃⁻) to active-site-labeled thrombins

Fitted dissociation constants and changes in fluorescence for binding of heparin and Hir-(54–65)(SO₃⁻) to the labeled thrombins in their free and complexed forms are summarized in Table 1. [4'F]FPR-T was previously shown to bind Hir-(54–65)(SO₃⁻) with 50% maximal fluorescence enhancement and $K_{T(Hir)} = 0.15 \mu$ M, approximately a 4-fold weaker affinity than that for unlabeled thrombin due to probe interference [40]. Heparin binding caused only a modest fluorescence quench, with heparin dependences up to 1 μ M being analyzed as single ligand interactions (Fig. 1A, inset) and dependences up to 200 μ M heparin showing biphasic behavior consistent with the presence of a weaker binding site (Fig. 1A). Similarly, [4'F]FPR-T exhibited only a 5% fluorescence quench on binding the exosite II ligand, F2 (Fig. 1B), with $K_{T(F2)} = 5 \pm 2 \mu$ M, indicating that the 4'F active site label is minimally perturbed by exosite II ligand binding.

[6F]FFR-T reported heparin binding to exosite II accompanied by 28% fluorescence quench. Binding to a weaker binding site was reported by a smaller 12% quench. Data up to 2 μM were analyzed as a single ligand interaction (Fig. 2A) and showed biphasic behavior at higher heparin concentrations (Fig. 2C). The affinity for tight heparin binding to [6F]FFR-T was modestly higher than that for binding to [4'F]FPR-T, whereas weak heparin binding was similar (Table 1). Hir-(54–65)(SO_3^-) binding to exosite I did not alter the fluorescence intensity of [6F]FFR-T in the absence of heparin, but it caused a reduction in fluorescence quench, $\Delta\Delta F/F_{\text{max}} = 0.13 \pm 0.01$, when bound to the [6F]FFR-T·Hep complex, with $K_{\text{T(Hep)(Hir)}} = 0.09 \pm 0.02 \mu\text{M}$ (Fig. 2B). Consistent reductions in fluorescence quench were observed in the heparin dependences at various fixed Hir-(54–65)(SO_3^-) concentrations (Fig. 2C). Fits by the models allowing (Fig. 2C, solid lines) and excluding (Fig. 2C, dashed lines) Hir-(54–65)(SO_3^-) binding to exosite I of the T·(Hep)₂ complex were very similar, with parameters listed in Table 1. Although the data were fit equally well by both models, the nonoverlapping model is in agreement with our previously published results of Hir-(54–65)(SO_3^-) binding to FPR-thrombin at 206 μM heparin, with $K_{\text{T(Hep)2(Hir)}} = 0.18 \pm 0.03 \mu\text{M}$ [16].

Fluorescence equilibrium binding of heparin, HCII, and the active-site-labeled thrombins in ternary or higher order complexes

In HCII dependences at various fixed heparin concentrations, [4'F]FPR-T reported hyperbolic saturating binding of HCII to exosite I in ternary and higher order complexes with heparin (Fig. 3A). The 50% fluorescence enhancement was identical to that observed in Hir-(54–65)(SO_3^-) binding to thrombin exosite I. Titration with AT at 5 μM heparin did not produce this enhancement, illustrating that HCII, but not AT, binds exosite I directly in the ternary complex. The anti-exosite II monoclonal antibody and low- M_r (5000) heparin significantly decreased the fluorescence enhancement (Fig. 3B), demonstrating the requirements of an accessible exosite II and a bridging heparin to form the ternary complex. Semi-logarithmic heparin dependences of the enhancement were bell-shaped, suggesting a template mechanism (Fig. 3C). [6F]FFR-T titrations with HCII at fixed heparin concentrations similarly reported saturating ternary and higher order complex formation (Fig. 4A), with absolute fluorescence intensity changes, reflecting an attenuation of fluorescence quench, expressed as $\Delta\Delta F/F_0$. Titration with AT at 1 μM heparin exhibited a smaller signal, indicating a weaker ternary complex. The heparin dependence of $\Delta\Delta F/F_0$ at 72 nM [6F]FFR-T and 0.38 μM HCII was also bell-shaped (Fig. 4B). The HCII and heparin dependences were fit adequately by the model including quaternary T·(Hep)₂HCII complex formation, whereas the model excluding this complex produced poor fits, with inconsistent K_D values for T·Hep, T·(Hep)₂, and HCII·Hep binding. The binding parameters for the respective ternary and quaternary complexes are listed in Table 1 and were in good agreement for both fluorescent thrombins. The difference in spacer arm and fluorescent label may contribute to modest variations in K_D for heparin binding and exosite I interactions. The HCII dependences exhibited saturation at heparin concentrations far below $K_{\text{HCII(Hep)}}$ for heparin binding to HCII, suggesting an ordered pathway of T·Hep binding to HCII. The ascending limb of the bell-shaped heparin dependences reflected saturation of the T·Hep complex and binding to HCII to produce maximal fluorescence change. The descending limb was the combined effect of T·(Hep)₂ binding to HCII and formation of the HCII·Hep complex, which binds to free thrombin and the T·Hep complex but much less so to the T·(Hep)₂ complex, presumably due to steric hindrance. The fits were consistent with $K_{\text{HCII(Hep)}} = 20 \pm 5 \mu\text{M}$, similar to the values reported independently by us and others [16,32]. Hir-(54–65)(SO_3^-) binding attenuated the affinity of the ternary [6F]FFR-T·Hep·HCII complex in a concentration-dependent manner (Fig. 4C), resulting in apparent $K_{\text{T(Hep)(HCII)}}$ values of 0.25 ± 0.03 and $1.3 \pm 0.1 \mu\text{M}$ at 25 and 250 nM Hir-(54–65)(SO_3^-), respectively, compared with $0.15 \pm 0.02 \mu\text{M}$ in the absence of peptide. This increase in

apparent $K_{T(\text{Hep})(\text{HCII})}$ was linear as a function of peptide concentration and illustrated competitive binding of the peptide and the HCII acidic domain to exosite I.

[5F]Hir-(54–65)(SO₃⁻) release from FPR-thrombin in the presence of heparin and HCII

Binding of 52 nM [5F]Hir-(54–65)(SO₃⁻) to 200 nM FPR-thrombin caused a 22% fluorescence quench, consistent with published data [49]. The fluorescence quench was unchanged by the addition of HCII, indicating that the FPR-thrombin interaction with HCII is weak in the absence of heparin. Titration of the FPR-thrombin/peptide/HCII mixture with heparin resulted in HCII- and heparin-dependent release of the peptide and a reduction of the fluorescence quench defined by the fractional fluorescence change $\Delta F/F_0$ (Fig. 5A). This signal change was saturated at heparin concentrations substantially below $K_{\text{HCII}(\text{Hep})}$, again demonstrating that formation of the T·Hep complex is a major pathway toward ternary complex formation. Analysis by the cubic equation for competitive binding of [5F]Hir-(54–65)(SO₃⁻) and HCII to the T·Hep complex, with $K_{T(\text{Hep})(\text{Hir})}$ fixed at 0.09 μM , gave $K_{T(\text{Hep})} = 0.50 \pm 0.20 \mu\text{M}$ for heparin binding to FPR-thrombin and $K_{T(\text{Hep})(\text{HCII})} = 0.60 \pm 0.20 \mu\text{M}$, in good agreement with the values for ternary complex formation reported in Table 1. Analysis by Eq. (3) gave $K_{T(\text{Hep})} = 0.60 \pm 0.20 \mu\text{M}$ and $K_{T(\text{Hep})(\text{HCII})} = 0.30 \pm 0.10 \mu\text{M}$, derived from the apparent ternary complex $K_D (0.90 \pm 0.10 \mu\text{M})$, including the competitive term $(1 + [P]_0/K_p)$ for [5F]Hir-(54–65)(SO₃⁻) binding to the T·Hep complex. This value is an approximation due to the fact that the concentrations of [5F]Hir-(54–65)(SO₃⁻) and the T·Hep complex are of the same order of magnitude, whereas the hyperbolic Eq. (3) was derived for conditions of $[\text{enzyme}]_0 < [P]_0, [\text{serpin}]_0$ [1].

The slightly downward curvature of the fit (Fig. 5A, dashed lines) reflects a small decrease in $[\text{HCII}]_{\text{free}}$ at higher heparin concentrations due to HCII·Hep complex formation. The heparin affinity for FPR-thrombin was modestly weaker than that for the fluorescently labeled thrombins, possibly due to the absence of the probe. Fluorescent peptide release was also observed in the formation of the ternary complex with AT; however, the signal change was smaller, suggesting that [5F]Hir-(54–65)(SO₃⁻) bound to exosite I poses less of a steric hindrance in formation of the encounter/Michaelis complex with AT than with HCII.

Effect of Hir-(54–65)(SO₃⁻) on the kinetics of heparin-accelerated thrombin inactivation by HCII

Hir-(54–65)(SO₃⁻) caused a hyperbolic decrease of the first-order inactivation rate constant k (Fig. 5B), approaching zero at high Hir-(54–65)(SO₃⁻) concentrations, suggesting negligible simultaneous peptide and HCII binding to exosite I during thrombin inactivation. Analysis of the data by Scheme 1 gave similar fitted $K_{T(\text{Hep})(\text{HCII})}$ values of $0.04 \pm 0.01 \mu\text{M}$ for the inactivation reactions at 1 and 50 μM heparin, demonstrating that the weak heparin binding did not interfere significantly with exosite I binding of the peptide or the HCII N-terminal acidic domain and suggesting that the lower k value in the reactions at 50 μM heparin, compared with 1 μM , is rather the result of a decrease in free HCII species required for ternary complex formation. Binding of HCII to the active T·Hep complex was 4- to 15-fold tighter than that to active-site-blocked T·Hep complexes, illustrating the concerted tightening action of HCII binding to the thrombin active site and exosite I, consistent with the tight binding of the ternary complex determined previously by kinetic analysis [16].

Stopped-flow kinetics of ternary complex formation between [6F]FFR-T, heparin, and HCII

Under our experimental conditions, stopped-flow traces of heparin binding to [6F]FFR-T were single exponentials with $k_{\text{obs}} = 26 \pm 1 \text{ s}^{-1}$, resulting in a 26% quench of the fluorescence intensity, consistent with the quenches observed in fluorescence equilibrium binding at similar heparin concentrations (Fig. 6). Reacting the binary complex of [6F]FFR-

T and heparin with HCII produced a single exponential with 15% fluorescence increase and $k_{\text{obs}} = 3.9 \pm 0.1 \text{ s}^{-1}$, whereas ternary complex formation by mixing [6F]FFR-T with a mixture of HCII and heparin was clearly biphasic, with the initial phase of the progress curve mirroring heparin binding to [6F]FFR-T with $k_{\text{obs1}} = 32 \pm 2 \text{ s}^{-1}$ and the second phase mirroring that of the T-Hep complex binding HCII with $k_{\text{obs2}} = 2.2 \pm 0.2 \text{ s}^{-1}$, consistent with the phases for both processes determined separately. These results suggest an ordered assembly of the ternary complex from the T-Hep binary complex and HCII and indicate that heparin binding to thrombin can be considered as a rapid equilibrium process. Our previous findings of a relatively slow limiting rate of approximately 0.1 s^{-1} for conversion of the Michaelis complex to the stable acyl-enzyme form [16] suggest that binding of active thrombin to heparin, and formation of the ternary complex with active thrombin, can indeed be considered as rapid equilibrium processes.

Discussion

This work presents quantitative binding studies characterizing the pathway of assembly of HCII, thrombin, and high- M_r heparin in ternary and higher order complexes. The catalytically inactive thrombin derivatives, [4'F]FPR-T and [6F]FFR-T, fluorescently labeled at the active site, respectively detected ligand interactions with exosites I and II while remaining essentially silent in reactions with the alternate exosite. This property greatly facilitated the analysis of fluorescence equilibrium binding and enabled selective monitoring of changes in each exosite environment on ligand binding in arrested encounter and Michaelis complexes, uncoupled from the chemical reactions of HCII cleavage and subsequent conformational changes associated with thrombin translocation in the acyl-enzyme. [6F]FFR-T also reported heparin binding to a second site on thrombin, and unlike free [6F]FFR-T, its complex with heparin did detect Hir-(54–65)(SO₃⁻) and HCII binding by comparable decreases in fluorescence quenching. Hir-(54–65)(SO₃⁻) and HCII binding to exosite I of [4'F]FPR-T caused comparable (~50%) fluorescence enhancements. Fluorescence intensity changes of the probes were the result of thermodynamic linkage between the thrombin active site and the exosites [41,42]. [6F]FFR-T was superior to the previously used probe, [6F]FPR-T, which detects both heparin and Hir-(54–65)(SO₃⁻) binding but with much smaller opposite fluorescence intensity changes [16].

The binding affinities of HCII and thrombin for heparin determine the order of assembly of ternary and higher order complexes. Heparin binding to HCII is 15 to 40 μM [16,17,32], significantly weaker than heparin binding to thrombin reported here and in previous work [1,15,16,18]. This results in thrombin saturation at heparin concentrations lower than $K_{\text{HCII(Hep)}}$, assuming rapid equilibrium binding of heparin to thrombin, illustrated by our stopped-flow results, and to HCII, as published previously [32]. The unique interaction of HCII acidic residues in the N-terminal 56-to-72 sequence with thrombin exosite I, absent in the thrombin-AT reaction, has been demonstrated by X-ray crystallography [26] and is described as the result of an allosteric mechanism in which heparin binding to HCII triggers a conformational change in the otherwise sequestered HCII N terminus [3,26]. Our equilibrium binding data demonstrate specific binding of HCII to exosite I under conditions where thrombin is saturated with heparin, suggesting that the allosteric reaction takes place in the pathway of T-Hep complex binding to HCII, with approximately a 100-fold higher affinity than HCII binding to heparin alone. The fluorescence stopped-flow results of alternate mixing are consistent with this hypothesis. This affinity of the T-Hep complex for HCII is increased even further, 4- to 15-fold, in reactions with active thrombin due to the concerted action of HCII binding to the active site and exosite I, as shown by our kinetic data of Hir-(54–65)(SO₃⁻) displacement during thrombin inactivation. Binding of the HCII

N-terminal sequence to thrombin exosite I in complexes with heparin was comparable to binding of Hir-(54–65)(SO₃⁻) to thrombin.

The affinity of a secondary weaker binding site for GAGs on thrombin was determined to be 5 to 6 μM for *M_r* 12,000 heparin and is likely to be dependent on the chain length and degree of sulfation [34,38]. Whereas the major binding site of heparin was identified in exosite II, the localization of the weaker binding site is unclear and was suggested to be in or near exosite I [21,36]; in a second subsite of exosite II, as illustrated by a recent crystal structure of sucrose octasulfate-bound thrombin [38]; or possibly identical to the GAG binding site we identified on the thrombin precursor, meizothrombin(des-fragment 1), in which exosite II is partially covered by fragment 2 [16].

Hir-(54–65)(SO₃⁻) binding to exosite I of heparin-saturated thrombin was characterized by $K_{T(Hep)(Hir)} = 0.09 \mu\text{M}$ and $K_{(Hep)_2(Hir)} = 0.15 \mu\text{M}$ (this study), comparable to 0.18 μM for [5F]Hir-(54–65)(SO₃⁻) binding to FPR-thrombin in the presence of 206 μM heparin [16]. These results indicate that exosite I is available for ligand and HCII binding when both heparin sites on thrombin are occupied. Similarly, analysis of the Hir-(54–65)(SO₃⁻) displacement from the T·Hep and T·(Hep)₂ complexes during thrombin inactivation by HCII suggested that the Hir-(54–65)(SO₃⁻) affinity was insignificantly affected by heparin binding to thrombin. The subtle weakening effect of heparin on peptide binding in the complexes with active-site-blocked thrombins may be related to conformational changes in exosite I caused by active site blocking, although active and active-site-blocked thrombins bound Hir-(54–65)(SO₃⁻) with similar affinity in the absence of heparin [11]. Whether heparin binding plays a role in invoking conformational changes in exosite I of active-site-blocked thrombin remains to be elucidated.

Whereas the uncatalyzed thrombin-AT reaction can still proceed at a 40 to 60% reduced rate in the presence of saturating Hir-(54–65)(SO₃⁻) [11], the heparin-accelerated thrombin-HCII reaction was decreased to approximately 5% of its original rate by 10 μM Hir-(54–65)(SO₃⁻) under our experimental conditions, strongly suggesting a competitive mechanism of Hir-(54–65)(SO₃⁻) and HCII binding to exosite I given the largely overlapping binding sites identified for Hir-(54–65)(SO₃⁻) and HCII on exosite I [24,26,55]. However, the lowest rates were still consistent with a second-order rate constant of approximately 0.2 μM⁻¹ s⁻¹, so it might be possible to have a small population of complexes in which simultaneous less efficient binding of Hir-(54–65)(SO₃⁻) and HCII binding to exosite I occurs. Tight binding of the T·Hep-HCII complex by high-*M_r* heparin bridging may favor the competitive mechanism given that the rate for thrombin reacting with sucrose octasulfate and HCII in a ternary complex decreased to approximately 33% of its original value at maximal experimental Hir-(54–65)(SO₃⁻) [34].

Data of [4'F]FPR-T and [6]FFR-T equilibrium binding to HCII and heparin in ternary and higher order complexes at high heparin concentration, where T·(Hep)₂ and HCII·Hep complexes are significantly and partially populated, respectively, were analyzed more consistently and produced better fits with the model that allows for HCII binding to T·(Hep)₂ and HCII·Hep binding to T and T·Hep but not to T·(Hep)₂. These observations challenge the suggestion that binding of heparin to two binding sites on thrombin may impair HCII binding to exosite I [39]. [6F]FFR-T also reported a 15% fluorescence quench for binding of high-*M_r* dermatan sulfate (DS) to exosite II [16], and its combination with [4'F]FPR-T may be equally useful for studying the assembly of thrombin and HCII in ternary and higher order complexes with DS. Heparin and DS bind different subsites in exosite II [56], and the geometry of DS bridging of thrombin and HCII may be different from that of heparin bridging, a hypothesis that was confirmed by a recently published

template model for DS binding [57]. These findings are consistent with previous studies of selective exosite II mutagenesis and exosite II ligand binding showing decreased efficiency of the heparin-catalyzed thrombin inactivation by HCII but lacking an effect on thrombin inactivation in the presence of DS [16,39,58]. The model reconciles a previous hypothesis of exclusively allosteric action of DS [39] with a template mechanism of DS for which we previously demonstrated evidence by kinetic and equilibrium binding studies [16]. Our binding studies with meizothrombin-(des-fragment 1) also suggested a DS binding site with $K_D \sim 6 \mu\text{M}$, on the periphery or perhaps outside of exosite II, which may be identical to, or overlapping with, the weak heparin binding site [16]. This binding site may be of importance in the DS-catalyzed mechanism given that no exosite II mutations that drastically decrease the DS-catalyzed inactivation by HCII have been identified. The quantitative mechanism-based analysis presented here will aid in further understanding the subtle differences in the thrombin-HCII interaction accelerated by diverse GAGs.

Acknowledgments

This project was supported by grant RO1 HL 080018 (I.M.V) from the National Heart, Lung, and Blood Institute of the National Institutes of Health. I thank Suryakala Sarilla and Sally Y. Habib for excellent technical assistance with purification and labeling of proteins, Paul Bock for providing [5F]Hir(54–65)(SO₃⁻), and Douglas Tollefsen for providing the anti-exosite II monoclonal antibody. The content of this article is solely the responsibility of the author and does not necessarily represent the official views of the National Heart, Lung, and Blood Institute or the National Institutes of Health.

References

1. Olson ST. Transient kinetics of heparin-catalyzed protease inactivation by antithrombin III. Linkage of protease-inhibitor-heparin interactions in the reaction with thrombin. *J Biol Chem.* 1988; 263:1698–1708. [PubMed: 3338989]
2. Tollefsen DM, Pestka CA, Monafu WJ. Activation of heparin cofactor II by dermatan sulfate. *J Biol Chem.* 1983; 258:6713–6716. [PubMed: 6687888]
3. Van Deerlin VM, Tollefsen DM. The N-terminal acidic domain of heparin cofactor II mediates the inhibition of alpha-thrombin in the presence of glycosaminoglycans. *J Biol Chem.* 1991; 266:20223–20231. [PubMed: 1939083]
4. Rogers SJ, Pratt CW, Whinna HC, Church FC. Role of thrombin exosites in inhibition by heparin cofactor II. *J Biol Chem.* 1992; 267:3613–3617. [PubMed: 1740413]
5. Mammen EF. Antithrombin: its physiological importance and role in DIC. *Semin Thromb Hemost.* 1998; 24:19–25. [PubMed: 9515776]
6. He L, Vicente CP, Westrick RJ, Eitzman DT, Tollefsen DM. Heparin cofactor II inhibits arterial thrombosis after endothelial injury. *J Clin Invest.* 2002; 109:213–219. [PubMed: 11805133]
7. Aihara K, Azuma H, Takamori N, Kanagawa Y, Akaike M, Fujimura M, Yoshida T, Hashizume S, Kato M, Yamaguchi H, Kato S, Ikeda Y, Arase T, Kondo A, Matsumoto T. Heparin cofactor II is a novel protective factor against carotid atherosclerosis in elderly individuals. *Circulation.* 2004; 109:2761–2765. [PubMed: 15148272]
8. Aihara K, Azuma H, Akaike M, Sata M, Matsumoto T. Heparin cofactor II as a novel vascular protective factor against atherosclerosis. *J Atheroscler Thromb.* 2009; 16:523–531. [PubMed: 19729870]
9. Noda A, Wada H, Kusiya F, Sakakura M, Onishi K, Nakatani K, Gabazza EC, Asahara N, Tsukada M, Nobori T, Shiku H. Plasma levels of heparin cofactor II (HCII) and thrombin-HCII complex in patients with disseminated intravascular coagulation. *Clin Appl Thromb Hemost.* 2002; 8:265–271. [PubMed: 12361205]
10. Kario K, Matsuo T, Kodama K, Katayama S, Kobayashi H. Preferential consumption of heparin cofactor II in disseminated intravascular coagulation associated with acute promyelocytic leukemia. *Thromb Res.* 1992; 66:435–444. [PubMed: 1412208]
11. Bock PE, Olson ST, Bjork I. Inactivation of thrombin by antithrombin is accompanied by inactivation of regulatory exosite I. *J Biol Chem.* 1997; 272:19837–19845. [PubMed: 9242645]

12. Thunberg L, Backstrom G, Lindahl U. Further characterization of the antithrombin-binding sequence in heparin. *Carbohydr Res.* 1982; 100:393–410. [PubMed: 7083257]
13. Olson ST, Swanson R, Raub–Segall E, Bedsted T, Sadri M, Petitou M, Hérault JP, Herbert JM, Bjork I. Accelerating ability of synthetic oligosaccharides on antithrombin inhibition of proteinases of the clotting and fibrinolytic systems. Comparison with heparin and low–molecular–weight heparin. *Thromb Haemost.* 2004; 92:929–939. [PubMed: 15543318]
14. Nordenman B, Danielsson A, Bjork I. The binding of low–affinity and high–affinity heparin to antithrombin. Fluorescence studies. *Eur J Biochem.* 1978; 90:1–6. [PubMed: 710412]
15. Streusand VJ, Bjork I, Gettins PG, Petitou M, Olson ST. Mechanism of acceleration of antithrombin–proteinase reactions by low affinity heparin. Role of the antithrombin binding pentasaccharide in heparin rate enhancement. *J Biol Chem.* 1995; 270:9043–9051. [PubMed: 7721817]
16. Verhamme IM, Bock PE, Jackson CM. The preferred pathway of glycosaminoglycan–accelerated inactivation of thrombin by heparin cofactor II. *J Biol Chem.* 2004; 279:9785–9795. [PubMed: 14701814]
17. Sarilla S, Habib SY, Tollefsen DM, Friedman DB, Arnett DR, Verhamme IM. Glycosaminoglycan–binding properties and kinetic characterization of human heparin cofactor II expressed in *Escherichia coli*. *Anal Biochem.* 2010; 406:166–175. [PubMed: 20670608]
18. Hogg PJ, Jackson CM. Heparin promotes the binding of thrombin to fibrin polymer. Quantitative characterization of a thrombin–fibrin polymer–heparin ternary complex. *J Biol Chem.* 1990; 265:241–247. [PubMed: 2294104]
19. Stubbs MT, Bode W. A player of many parts: the spotlight falls on thrombin's structure. *Thromb Res.* 1993; 69:1–58. [PubMed: 8465268]
20. Bode W, Turk D, Karshikov A. The refined 1.9–Å X–ray crystal structure of D–Phe–Pro–Arg chloromethylketone–inhibited human alpha–thrombin: structure analysis, overall structure, electrostatic properties, detailed active–site geometry, and structure–function relationships. *Protein Sci.* 1992; 1:426–471. [PubMed: 1304349]
21. Naski MC, Fenton JW 2nd, Maraganore JM, Olson ST, Shafer JA. The COOH–terminal domain of hirudin. An exosite–directed competitive inhibitor of the action of alpha–thrombin on fibrinogen. *J Biol Chem.* 1990; 265:13484–13489. [PubMed: 2380171]
22. Hortin GL, Tollefsen DM, Benutto BM. Antithrombin activity of a peptide corresponding to residues 54–75 of heparin cofactor II. *J Biol Chem.* 1989; 264:13979–13982. [PubMed: 2760054]
23. Ragg H, Ulshofer T, Gerewitz J. Glycosaminoglycan–mediated leuserpin–2/thrombin interaction. Structure–function relationships. *J Biol Chem.* 1990; 265:22386–22391. [PubMed: 2266131]
24. Myles T, Church FC, Whinna HC, Monard D, Stone SR. Role of thrombin anion–binding exosite–I in the formation of thrombin–serpin complexes. *J Biol Chem.* 1998; 273:31203–31208. [PubMed: 9813026]
25. Mitchell JW, Church FC. Aspartic acid residues 72 and 75 and tyrosine–sulfate 73 of heparin cofactor II promote intramolecular interactions during glycosaminoglycan binding and thrombin inhibition. *J Biol Chem.* 2002; 277:19823–19830. [PubMed: 11856753]
26. Baglin TP, Carrell RW, Church FC, Esmon CT, Huntington JA. Crystal structures of native and thrombin–complexed heparin cofactor II reveal a multistep allosteric mechanism. *Proc Nat Acad Sci USA.* 2002; 99:11079–11084. [PubMed: 12169660]
27. Gan ZR, Li Y, Chen Z, Lewis SD, Shafer JA. Identification of basic amino acid residues in thrombin essential for heparin–catalyzed inactivation by antithrombin III. *J Biol Chem.* 1994; 269:1301–1305. [PubMed: 8288594]
28. Sheehan JP, Sadler JE. Molecular mapping of the heparin–binding exosite of thrombin. *Proc Nat Acad Sci USA.* 1994; 91:5518–5522. [PubMed: 8202520]
29. Colwell NS, Grupe MJ, Tollefsen DM. Amino acid residues of heparin cofactor II required for stimulation of thrombin inhibition by sulphated polyanions. *Biochim Biophys Acta.* 1999; 1431:148–156. [PubMed: 10209287]
30. Ersdal–Badju E, Lu A, Zuo Y, Picard V, Bock SC. Identification of the antithrombin III heparin binding site. *J Biol Chem.* 1997; 272:19393–19400. [PubMed: 9235938]

31. Li W, Johnson DJ, Esmon CT, Huntington JA. Structure of the antithrombin–thrombin–heparin ternary complex reveals the antithrombotic mechanism of heparin. *Nat Struct Mol Biol.* 2004; 11:857–862. [PubMed: 15311269]
32. O’Keeffe D, Olson ST, Gasiunas N, Gallagher J, Baglin TP, Huntington JA. The heparin binding properties of heparin cofactor II suggest an antithrombin–like activation mechanism. *J Biol Chem.* 2004; 279:50267–50273. [PubMed: 15371417]
33. Li EH, Orton C, Feinman RD. The interaction of thrombin and heparin. Proflavine dye binding studies. *Biochemistry.* 1974; 13:5012–5017. [PubMed: 4373048]
34. Sarilla S, Habib SY, Kravtsov DV, Matafonov A, Gailani D, Verhamme IM. Sucrose octasulfate selectively accelerates thrombin inactivation by heparin cofactor II. *J Biol Chem.* 2010; 285:8278–8289. [PubMed: 20053992]
35. Machovich R, Aranyi P. Effect of heparin on thrombin inactivation by antithrombin–III. *Biochem J.* 1978; 173:869–875. [PubMed: 708377]
36. Olson ST, Halvorson HR, Bjork I. Quantitative characterization of the thrombin–heparin interaction. Discrimination between specific and nonspecific binding models. *J Biol Chem.* 1991; 266:6342–6352. [PubMed: 2007587]
37. Fenton JW 2nd, Witting JI, Pouliott C, Fareed J. Thrombin anion–binding exosite interactions with heparin and various polyanions. *Ann NY Acad Sci.* 1989; 556:158–165. [PubMed: 2660684]
38. Desai BJ, Boothello RS, Mehta AY, Scarsdale JN, Wright HT, Desai UR. Interaction of thrombin with sucrose octasulfate. *Biochemistry.* 2011; 50:6973–6982. [PubMed: 21736375]
39. Sheehan JP, Tollefsen DM, Sadler JE. Heparin cofactor II is regulated allosterically and not primarily by template effects. Studies with mutant thrombins and glycosaminoglycans. *J Biol Chem.* 1994; 269:32747–32751. [PubMed: 7806495]
40. Verhamme IM, Olson ST, Tollefsen DM, Bock PE. Binding of exosite ligands to human thrombin. Re–evaluation of allosteric linkage between thrombin exosites I and II. *J Biol Chem.* 2002; 277:6788–6798. [PubMed: 11724802]
41. Bock PE. Active–site–selective labeling of blood coagulation proteinases with fluorescence probes by the use of thioester peptide chloromethyl ketones. II. Properties of thrombin derivatives as reporters of prothrombin fragment 2 binding and specificity of the labeling approach for other proteinases. *J Biol Chem.* 1992; 267:14974–14981. [PubMed: 1634536]
42. Bock PE. Active–site–selective labeling of blood coagulation proteinases with fluorescence probes by the use of thioester peptide chloromethyl ketones. I. Specificity of thrombin labeling. *J Biol Chem.* 1992; 267:14963–14973. [PubMed: 1634535]
43. Olson ST, Bjork I, Shore JD. Kinetic characterization of heparin–catalyzed and uncatalyzed inhibition of blood coagulation proteinases by antithrombin. *Methods Enzymol.* 1993; 222:525–559. [PubMed: 8412815]
44. Chase T Jr, Shaw E. Comparison of the esterase activities of trypsin, plasmin, and thrombin on guanidinobenzoate esters. Titration of the enzymes. *Biochemistry.* 1969; 8:2212–2224. [PubMed: 4239491]
45. Fenton JW 2nd, Fasco MJ, Stackrow AB. Human thrombins. Production, evaluation, and properties of alpha–thrombin. *J Biol Chem.* 1977; 252:3587–3598. [PubMed: 16908]
46. Mann KG, Elion J, Butkowski RJ, Downing M, Nesheim ME. Prothrombin. *Methods Enzymol.* 1981; 80(Pt C):286–302. [PubMed: 7043193]
47. Church FC, Meade JB, Pratt CW. Structure–function relationships in heparin cofactor II: spectral analysis of aromatic residues and absence of a role for sulfhydryl groups in thrombin inhibition. *Arch Biochem Biophys.* 1987; 259:331–340. [PubMed: 3426230]
48. Colwell NS, Blinder MA, Tsiang M, Gibbs CS, Bock PE, Tollefsen DM. Allosteric effects of a monoclonal antibody against thrombin exosite II. *Biochemistry.* 1999; 38:2610. [PubMed: 10029715]
49. Anderson PJ, Nasset A, Dharmawardana KR, Bock PE. Characterization of proexosite I on prothrombin. *J Biol Chem.* 2000; 275:16428–16434. [PubMed: 10748007]
50. Tian WX, Tsou CL. Determination of the rate constant of enzyme modification by measuring the substrate reaction in the presence of the modifier. *Biochemistry.* 1982; 21:1028–1032. [PubMed: 7074045]

51. Hogg PJ, Jackson CM. Fibrin monomer protects thrombin from inactivation by heparin–antithrombin III: implications for heparin efficacy. *Proc Nat Acad Sci USA*. 1989; 86:3619–3623. [PubMed: 2726739]
52. Lottenberg R, Christensen U, Jackson CM, Coleman PL. Assay of coagulation proteases using peptide chromogenic and fluorogenic substrates. *Methods Enzymol*. 1981; 80(Pt C):341–361. [PubMed: 6210826]
53. Dharmawardana KR, Olson ST, Bock PE. Role of regulatory exosite I in binding of thrombin to human factor V, factor Va, factor Va subunits, and activation fragments. *J Biol Chem*. 1999; 274:18635–18643. [PubMed: 10373475]
54. Verhamme IM, Bock PE. Rapid–reaction kinetic characterization of the pathway of streptokinase–plasmin catalytic complex formation. *J Biol Chem*. 2008; 283:26137–26147. [PubMed: 18658146]
55. Bock PE, Panizzi IM, Verhamme, Exosites in the substrate specificity of blood coagulation reactions. *J Thromb Haemost*. 2007; 1(5 Suppl):81–94. [PubMed: 17635714]
56. Tollefsen DM. The interaction of glycosaminoglycans with heparin cofactor II. *Ann NY Acad Sci*. 1994; 714:21–31. [PubMed: 8017769]
57. Raghuraman A, Mosier PD, Desai UR. Understanding dermatan sulfate– heparin cofactor II interaction through virtual library screening. *ACS Med Chem Lett*. 2010; 1:281–285. [PubMed: 20835364]
58. Liaw PC, Austin RC, Fredenburgh JC, Stafford AR, Weitz JI. Comparison of heparin– and dermatan sulfate–mediated catalysis of thrombin inactivation by heparin cofactor II. *J Biol Chem*. 1999; 274:27597–27604. [PubMed: 10488098]

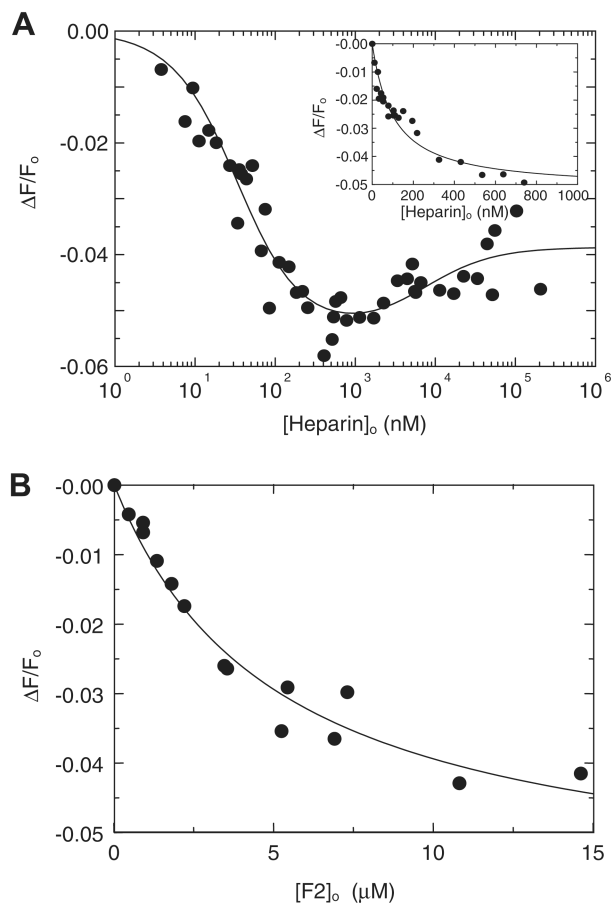
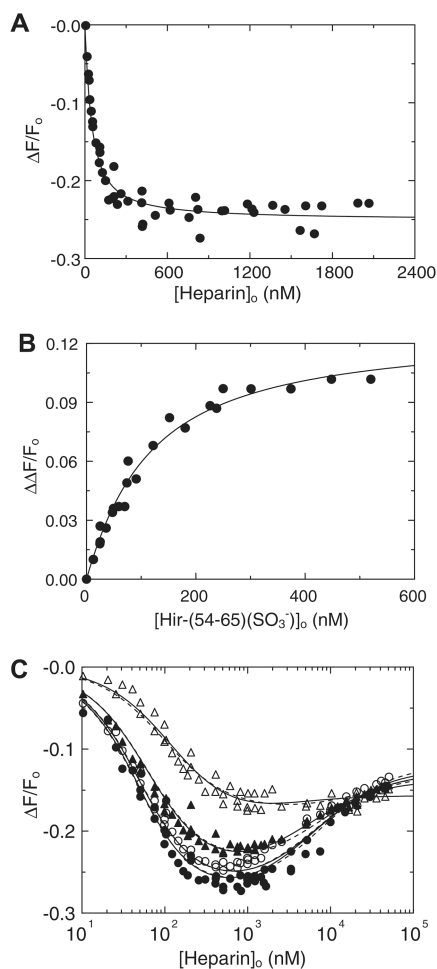
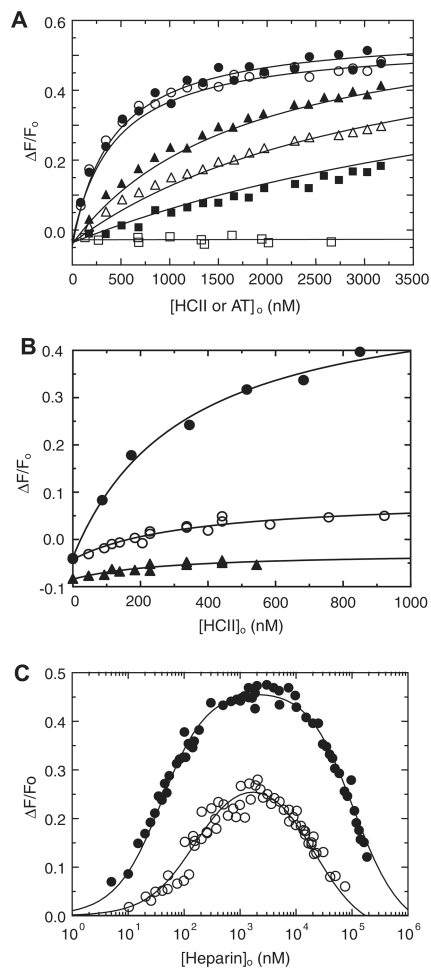


Fig.1. Fluorescence equilibrium binding of heparin and F2 to $[4'F]\text{FPR-T}$. (A) Fractional change in fluorescence ($\Delta F/F_0$) of 10 nM $[4'F]\text{FPR-T}$ as a function of total heparin concentration ($[\text{Heparin}]_0$). The solid line represents least squares fits of the data by Eq. (1). Inset: $\Delta F/F_0$ as a function of total heparin concentration, up to 1 μM , analyzed by the quadratic equation for binding of a single ligand. (B) Fractional change in fluorescence ($\Delta F/F_0$) of 10 nM $[4'F]\text{FPR-T}$ as a function of total F2 concentration ($[\text{F2}]_0$), analyzed by the quadratic equation for binding of a single ligand. Fitted parameters are listed in Results and in Table 1.

**Fig.2.**

Fluorescence equilibrium binding of heparin to [6F]FFR-T and the effect of Hir-(54–65)(SO₃⁻). (A) Fractional change in fluorescence ($\Delta F/F_0$) of 20 nM [6F]FFR-T as a function of total heparin concentration up to 2 IM ($[\text{Heparin}]_0$). (B) Absolute fractional change in fluorescence ($\Delta\Delta F/F_0$) of 35 nM [6F]FFR-T in the presence of 1.56 IM heparin as a function of total Hir-(54–65)(SO₃⁻) concentration ($[\text{Hir-(54-65)(SO}_3^-)]_0$). Solid lines represent least squares fits of the data by the quadratic equation for binding of a single ligand. (C) Fractional change in fluorescence ($\Delta F/F_0$) of 35 nM [6F]FFR-T in the presence of 0 (●), 5 (○), 25 (▲), and 250 (Δ) nM Hir-(54–65)(SO₃⁻) as a function of total heparin concentration ($[\text{Heparin}]_0$), reflecting tight and weak heparin binding sites of heparin on thrombin. Solid and dashed lines represent least squares fits of the data respectively by models for nonoverlapping and competitive binding of Hir-(54–65)(SO₃⁻) to exosite I and heparin to the weak binding site. Fitted parameters are listed in Table 1.

**Fig.3.**

Fluorescence equilibrium binding of heparin and F2 to $[4'F]FPR-T$. (A) Fractional change in fluorescence ($\Delta F/F_0$) of 10 nM $[4'F]FPR-T$ as a function of total heparin concentration ($[Heparin]_0$). The solid line represents least squares fits of the data by Eq. (1). Inset: $\Delta F/F_0$ as a function of total heparin concentration, up to 1 μM , analyzed by the quadratic equation for binding of a single ligand. (B) Fractional change in fluorescence ($\Delta F/F_0$) of 10 nM $[4'F]FPR-T$ as a function of total F2 concentration ($[F2]_0$), analyzed by the quadratic equation for binding of a single ligand. Fitted parameters are listed in Results and in Table 1.

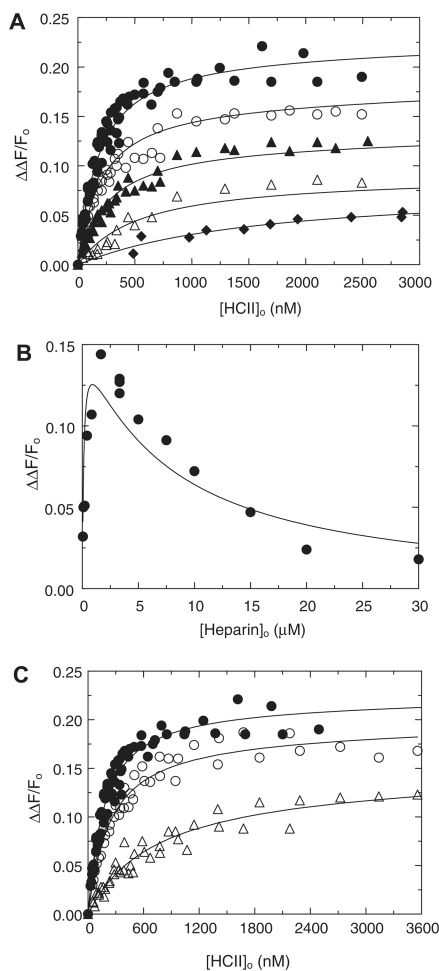
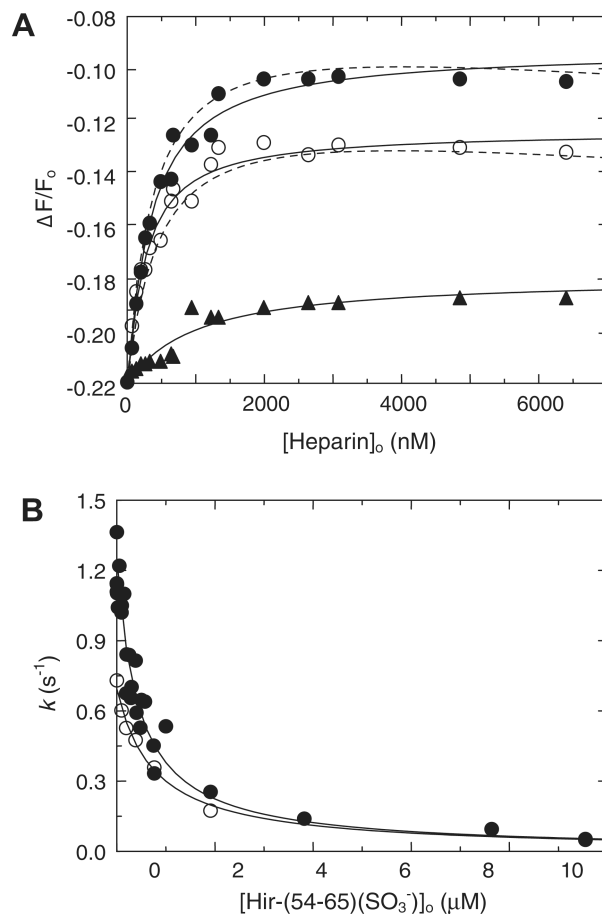


Fig.4. Fluorescence equilibrium binding of [6F]FFR-T, heparin, and HCII in ternary and quaternary complexes. (A) Absolute fluorescence change ($\Delta\Delta F/F_0$) of 35 nM [6F]FFR-T as a function of total HCII concentration ($[HCII]_0$), with HCII dependences at 1.6 (●), 5.2 (○), 13.5 (▲), and 47 (△) μM heparin and a titration with AT at 0.22 μM heparin (◆). (B) Heparin dependence of $\Delta\Delta F/F_0$ of 72 nM [6F]FFR-T in the presence of 0.38 μM HCII. Solid lines represent least squares fits by the model for ternary and quaternary complex formation, with parameters listed in Table 1. (C) Effect of 25 (○) and 250 (△) nM Hir-(54–65)(SO_3^-) on the HCII dependence at 1.6 μM heparin (●, from panel A). Solid lines represent fits by the ternary complex formation model, predominant at 1.6 μM heparin, with parameters listed in Results.

**Fig.5.**

Displacement of Hir-(54–65)(SO₃⁻) from FPR-thrombin and active thrombin during ternary complex formation with HCII and heparin. (A) Fractional fluorescence change ($\Delta F/F_0$) of the complex of [5F]Hir-(54–65)(SO₃⁻) with FPR-thrombin (45 nM complex) as a function of total heparin concentration ($[\text{Heparin}]_0$) in the presence of 0.9 (●) and 1.5 (○) μM HCII and 0.5 μM AT (▲). Solid lines (HCII) are fits by the cubic equation for competitive binding of the peptide and HCII to the T·Hep complex and by the quadratic equation for the heparin dependence of the AT reaction. Dashed lines are fits by Eq. (3). (B) Hir-(54–65)(SO₃⁻) dependence of the decrease of the first-order inactivation rate constant k of thrombin inactivation by HCII at 1 (●) and 50 (○) μM heparin. Experiments were analyzed as described in Materials and Methods, and parameters are listed in Results.

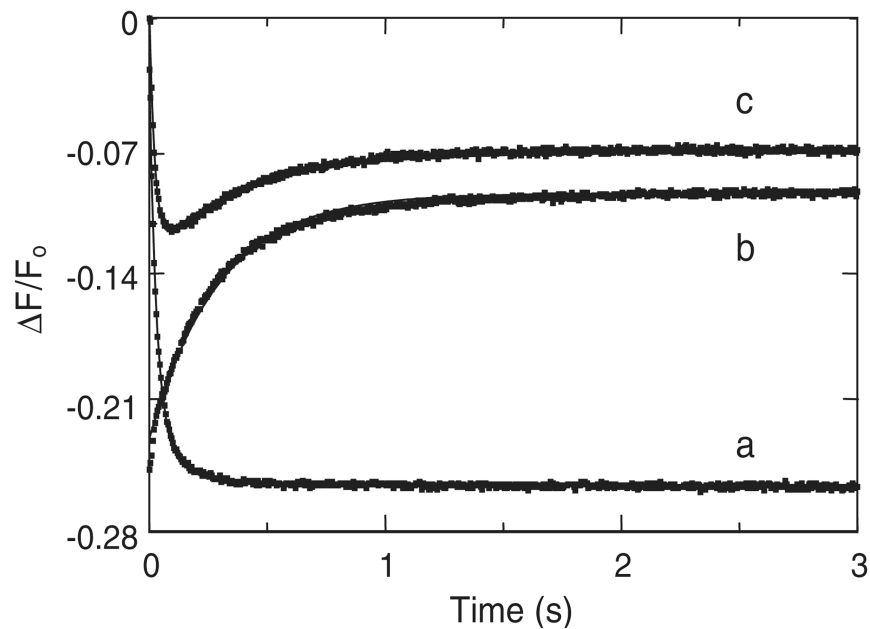
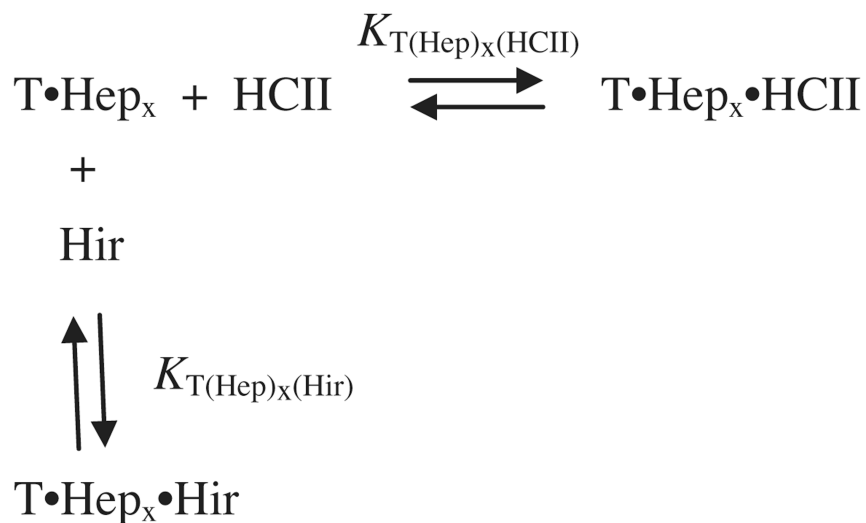


Fig.6. Order of assembly of [6F]FFR-T, HCII, and heparin in a ternary complex. Stopped-flow traces of [6F]FFR-T reacting with heparin (a), of a [6F]FFR-T/heparin mixture reacting with HCII (b), and of [6F]FFR-T reacting with an HCII/heparin mixture (c). Curves were analyzed as mono- and biexponential time dependences of fluorescence change, as described in Materials and Methods.

**Scheme 1.**

Competition of HCII and the peptide for exosite I. Mutually exclusive binding of HCII and Hir-(54–65)(SO₃⁻) to the thrombin·(heparin)_x complex. HCII and Hir-(54–65)(SO₃⁻) (*Hir*) compete for binding to exosite I of the thrombin·(heparin)_x complex (T·Hep_x) in which x represents 1 or 2 molecules of heparin bound to thrombin. The dissociation constants for the higher order complexes with HCII or Hir-(54–65)(SO₃⁻) are $K_{T(\text{Hep})_x(\text{HCII})}$ and $K_{T(\text{Hep})_x(\text{Hir})}$, respectively.

Table 1

Parameters for heparin, Hir-(54-65)(SO₃⁻), and HCII binding to fluorescent thrombins.

		K_D (μM)	$\Delta F_{\text{max}}/F_0$ (%)
[4'F]FPR-T			
Heparin binding	$K_{\text{T(Hep)}}$	$0.10 \pm 0.02^{a,b}$	-5 ± 1
		0.40 ± 0.06^c	-6 ± 1
	$K_{\text{T(Hep)2}}$	3 ± 4^b	-4 ± 1
		7 ± 1^c	-4 ± 1
Hir-(54-65)(SO ₃ ⁻) binding	$K_{\text{T(Hir)}}$	$0.15 \pm 0.02^{a,d}$	50 ± 2
	T-Hep-HCII complex	$0.23 \pm 0.03^{c,e}$	54 ± 2
T-Hep-HCII complex	$K_{\text{T(Hep)(HCII)}}$	$0.20 \pm 0.02^{c,f}$	51 ± 2
		$0.60 \pm 0.14^{c,e}$	66 ± 6
T-(Hep) ₂ -HCII complex	$K_{\text{T(Hep)2(HCII)}}$	$0.60 \pm 0.10^{c,f}$	54 ± 6
[6F]FFR-T			
Heparin binding	$K_{\text{T(Hep)}}$	$0.03 \pm 0.01^{a,b}$	-28 ± 1
		6 ± 2^b	-12 ± 2
	$K_{\text{T(Hep)2}}$	7 ± 2^c	-7 ± 2
		7 ± 2^g	-12 ± 1
		5 ± 1^h	-13 ± 1
$K_{\text{T(Hir)(Hep)}}$	0.20 ± 0.05^g	-13 ± 6	
Hir-(54-65)(SO ₃ ⁻) binding	$K_{\text{T(Hir)}}$	0.09 ± 0.02^h	-14 ± 1
		$0.03 \pm 0.01^{g,h}$	0
	$K_{\text{T(Hep)(Hir)}}$	0.10 ± 0.02^a	-15 ± 2
	$K_{\text{T(Hep)2(Hir)}}$	0.15 ± 0.05^g	-16 ± 2
	T-Hep-HCII complex	$K_{\text{T(Hep)(HCII)}}$	$0.15 \pm 0.02^{c,e}$
$0.30 \pm 0.06^{c,f}$			-6 ± 1
T-(Hep) ₂ -HCII complex	$K_{\text{T(Hep)2(HCII)}}$	$0.14 \pm 0.03^{c,e,f}$	-7 ± 2

Note. Dissociation constants (K_D) and fluorescence intensity changes ($\Delta F_{\text{max}}/F_0$) for heparin and Hir-(54-65)(SO₃⁻) binding to [4'F]FPR-T and [6F]FFR-T, and for the ternary and quaternary complexes with HCII, were determined by equilibrium binding. Experiments were performed and analyzed as described in Materials and Methods. Errors represent ± 2 standard deviations.

^aQuadratic binding of a single ligand.

^bEq. (1).

^cModel of ternary and quaternary complex formation with HCII.

^dPublished data [40].

^eFrom the HCII dependence.

^fFrom the heparin dependence.

^gNonoverlapping second heparin and Hir-(54–65)(SO₃⁻) binding.

^hCompetitive second heparin and Hir-(54–65)(SO₃⁻) binding.